Journal of Materials Chemistry A

Accepted Manuscript

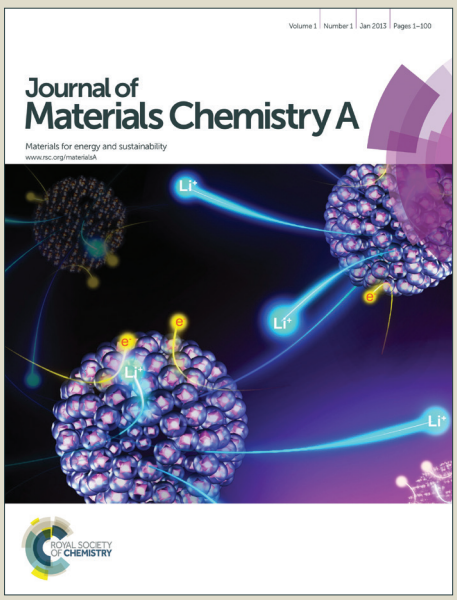

ROYAL SOCIETY OF CHEMISTRY

www.rsc.org/materialsA

Synthesis and Photovoltaic Properties of An n-Type Two-Dimension-Conjugated Polymer Based on Perylene Diimide and Benzodithiophene with Thiophene Conjugated Side Chains

Youdi Zhang,[a] Qun Wan,[a] Xia Guo,[a]* Wanbin Li,[a] Bing Guo,[a] Maojie Zhang,[a]* Yongfang Li [ab]*

[a] Laboratory of Advanced Optoelectronic Materials, College of Chemistry, Chemical Engineering and Materials Science, Soochow University, Suzhou 215123, China.

E-mail: mjzhang@suda.edu.cn, guoxia@suda.edu.cn

[b] Beijing National Laboratory for Molecular Sciences, CAS Key Laboratory of Organic Solids, Institute of Chemistry, Chinese Academy of Sciences, Beijing 100190, China.

E-mail: liyf@iccas.ac.cn

Keywords: perylene diimides; n-type 2D-conjugated polymer; acceptor materials; all-polymer solar cells

Abstract:

A novel n-type two-dimension (2D)-conjugated polymer based on bithienyl-benzodithiophene (BDT) and perylene diimide (PDI), **P(PDI-BDT-T)**, is synthesized by Stille coupling reaction for the application as acceptor material in all-polymer solar cells (PSCs). **P(PDI-BDT-T)** exhibits broad absorption in visible region with the optical bandgap (E_g) of 1.64 eV, and a LUMO level of -3.89 eV which is similar with and slightly higher than that of PCBM, indicating that the polymer is

suitable for the application as acceptor instead of PCBM in PSCs. The PSCs with **P(PDI-BDT-T)** as aceptor and PTB7-Th as donor demonstrated a power conversion efficiency (PCE) of 4.71% with a J_{sc} of 11.51 mA cm^{-2}, V_{oc} of 0.80 V, and FF of 51.1%. While the PCE of the PSCs based on the acceptor of a corresponding 1D-conjugated polymer P(PDI-BDT-O) with alkoxy side chain on BDT unit was only 2.75% with a J_{sc} of 10.14 mA cm^{-2}, V_{oc} of 0.72 V, and FF of 37.6%. These results indicate that the 2D-conjugated **P(PDI-BDT-T)** is a promising acceptor material for all polymer PSCs.

Introduction

All-polymer solar cells (all-PSCs), composed of a *p*-type conjugated polymer as donor and a *n*-type conjugated polymer as acceptor, have attracted much attention recently, due to the potential advantages of *n*-type conjugated polymer acceptors over the traditional fullerene derivative PCBM on easy-tuning absorption spectra and electronic energy levels as well as better flexibility.[1-25] One of the challenges for all-PSCs is the development of effective *n*-type conjugated polymers. Perylene diimide (PDI) is a typical *n*-type organic semiconductor, and a *n*-type conjugated polymer based on PDI unit was first reported for all PSCs in 2007 by Zhan *et al*[4] and a power conversion efficiency (PCE) of 1.50% was obtained for the all-PSCs with the polymer as acceptor and a two-dimension (2D)-conjugated polythiophene derivative with conjugated side chain as donor.[5] Zhou *et al* then synthesized a series of *n*-type conjugated polymers based on PDI and several donor units and PCE of over 2% was

achieved for all-PSCs with the *n*-type polymers as acceptor.[6] In 2014, the PCE of all-PSCs based on PDI containing polymers reached up to 4.4% reported by Bao *et al*, [26] which is the highest performance in published literatures for all-PSCs based on PDI system so far. Now, PDI-based polymers have become representative *n*-type conjugated polymers for all-PSCs.

In recent years, two dimension (2D) conjugated polymers based on benzodithiophene unit have received much attention for the application as donor materials in PSCs, because of their advantages of better light absorption, higher thermal stabilities, deeper highest occupied molecular orbital (HOMO) level, higher hole mobilities and better photovoltaic performance.[27-35] But, there is no *n*-type 2D-conjugated polymers reported for the application as acceptor in PSCs till now. In order to extend the concept of 2D conjugated polymers to the *n*-type polymers and study the effect of the conjugated side chains on the photovoltaic performance of the *n*-type polymer acceptor, we designed and synthesized a *n*-type 2D-conjugated D-A copolymer **P(PDI-BDT-T)** based on thienyl substituted benzodithiophene (BDT) as donor (D) unit and PDI as acceptor (A) unit by Stille coupling polymerization. Meanwhile, a corresponding n-type 1D-conjugated polymer P(PDI-BDT-O) with alkoxy substituent on BDT unit was also synthesized for comparison (**Fig. 1**). **P(PDI-BDT-T)** exhibits broad absorption in visible light range with a optical bandgap (E_g) of 1.64 eV, which will enhance the light harvesting of the active layer when it is used as acceptor material. Furthermore, **P(PDI-BDT-T)** shows a LUMO level of -3.89 eV which is similar with and slightly higher than that of PCBM, indicating the

potential feasibility for its application as acceptor instead of PCBM from the energy level of view. The photovoltaic performance of the all-PSCs based on **P(PDI-BDT-T)** as acceptor and PTB7-Th as donor demonstrated a higher PCE of 4.71% with a J_{sc} of 11.51 mA cm^{-2}, V_{oc} of 0.80 V, and FF of 51.1%. While the PCE of the all-PSCs with P(PDI-BDT-O) as acceptor was only 2.75% with a J_{sc} of 10.14 mA cm^{-2}, V_{oc} of 0.72 V, and FF of 37.6%, indicating that the 2D structure of the n-type conjugated polymers is also superior to the corrsponding 1D polymer for the application as acceptors in all-PSCs.

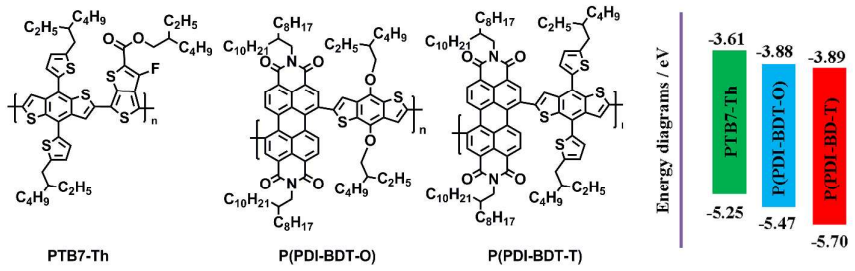

Fig. 1 Molecular structures and energy levels of PTB7-Th, P(PDI-BDT-O) and **P(PDI-BDT-T)**.

Experimental

Synthesis of P(PDI-BDT-T)

Monomers 2Br-PDI[36-39] BDT-T[40] and BDT-O[41] were prepared by using experimental procedures reported in literatures. It should be mentioned that monomer 2Br-PDI is a mixture of 1,7 and 1,6 regioisomers, and their ratio is ca. 5:1 according to the ^{1}H-NMR spectrum of dibro-Perylene-3,4,9,10-tetracarboxylic dianhydride (2Br-PDI) (see Figure S1 in Supplementary Information (SI)). The synthesis processes of polymer **P(PDI-BDT-T)** are as follows:

2Br-PDI (300 mg, 0.27 mmol), BDT-T (245 mg, 0.27 mmol) and $Pd(PPh_3)_4$ (18.8 mg, 0.016 mmol) were added into a 50 mL three-neck round-bottom flask with 10 mL toluene solution. The flask equipped with a return pipe was then degassed and filled with argon for three times. The reaction mixture was treated for 48 h under argon atmosphere. After cooling, the reaction solution was added into 100 mL methanol. Subsequently, the polymer was precipitated as a dark reddish solid, dried in vacuum drying oven, and then purified by Soxhlet extraction with methanol, acetone, and hexane. **P(PDI-BDT-T)** (300 mg; 71%), Anal. Calcd for $C_{98}H_{128}N_2O_4S_4$ (%): C 77.12, H 8.45, N 1.84, O 4.19, S, 8.40; found (%): C 76.43, H 8.40, N 1.77, O 4.31, S 9.09; ^{1}H NMR (400 MHz, $CDCl_3$) δ 8.82 (d, 1H), 8.48 (s, 1H), 8.39 (d, 1H), 8.05 – 7.89 (m, 1H), 7.29 (d, 1H), 6.81 (s, 1H), 4.12 (s, 2H), 2.79 (d, 2H), 2.01 (s, 1H), 1.55 – 0.71 (m, 66H).

The polymer P(PDI-BDT-O) was synthesized by similar synthetic procedures as that of synthesizing **P(PDI-BDT-T)**: 2Br-PDI (330 mg, 0.30 mmol), BDT-O (230 mg, 0.30 mmol) and $Pd(PPh_3)_4$ (21 mg, 0.018 mmol), P(PDI-BDT-O) (157 mg; 37%), ^{1}H NMR (400 MHz, $CDCl_3$) δ 8.92 (s, 1H), 8.36 (t, 2H), 7.79 (d, 1H), 4.24 (s, 4H), 2.02 (s, 1H), 1.76 (s, 1H), 1.40 (d, 42H), 0.80 (d, 14H).

Instruments and Measurements

Absorption spectra were taken on a Cary-5000 UV-vis Spectrophotometer in chloroform solution and in thin film. Electrochemical cyclic voltammetry was measured on a Zahner IM6e Electrochemical Workstation with a Platinum-carbon as working electrode, a Pt wire as auxiliary electrode, and a Ag/Ag^+ electrode as

reference electrode, in a 0.1 mol L^{-1} tetrabutylammonium hexafluorophosphate (Bu_4NPF_6) acetonitrile electrolyte solution. The AFM measurement of the surface morphology of blend films was carried out on a Nanoscope III (DI, USA) in contact mode with 5 μm scanners. And TEM images of active layers were taken by using Tecnai G2F20 (FEI, USA).

Charge carrier mobility

The charge carrier mobility was measured by the space charge limited current (SCLC) method with the structure of ITO/PEDOT:PSS/Active layer/Au (hole-only device) for the hole mobility measurement or with the structure of ITO/Al/Active layer/Al (electron-only device) for the electron mobility measurement. After measurements of the *J-V* curves of the devices, the hole mobilities and the electron mobilities were calculated roughly by the following equation,

$$J = \frac{8}{9}\varepsilon_r \varepsilon_0 \mu_e \frac{V^2}{L^3}$$

where ε_r is the dielectric constant of the polymer, ε_0 is the permittivity of the vacuum, μ_0 is the zero-field mobility, J is the current density, L is the thickness of the blend films, $V = V_{appl} - V_{bi}$, V_{appl} is the applied potential, and V_{bi} is the built-in potential from the difference in the work function of the anode and the cathode (in the hole-only and electron-only device, V_{bi} value is 0.2 V and 0 V respectively).

Device fabrication and characterization

The ITO-coated glass substrate was cleaned in an ultrasonic bath with deionized water, acetone, and isopropanol, each process was approximately 20 min, and then dried under a stream of dry nitrogen. Subsequently, the ITO-coated glass

substrate was treated by UV-ozone for 20 min. PEDOT:PSS (Clevios P VP AI 4083, H.C. Starck) solution was then spin-coated onto the pre-cleaned ITO coated glass substrates, and thermal-treated at 150 ^{o}C for 15 min to get the PEDOT:PSS film with thickness of ~40 nm.

The blend solutions of PTB7-Th and **P(PDI-BDT-T)** were prepared by simultaneously dissolving PTB7-Th and **P(PDI-BDT-T)** with D/A weight ratio of 2:1, 1.5:1 and 1:1 respectively, in dichlorobenzene with or without solvent additives (DIO, CN and NMP), and spin-coated on the ITO/PEDOT: PSS electrode at 2000 rpm for 30 s. The active layers were treated by thermal annealing at 100 °C and 120 °C for 10 min in nitrogen condition, respectively, resulting in the active layer with a film thickness of ~90 nm. Then 20 nm thick Ca layer covered with 100 nm Al electrode were thermally deposited under a pressure of 2×10^{-4} Pa, through a shadow mask on top of the active layer. The active area of the pixels, as defined by the overlap of anode and cathode area, was 0.04 cm^2. The thickness was measured by Ambios Technology D-100 surface profilometer. The current density-voltage (*J-V*) curves were measured in N_2 atmosphere using AM 1.5G solar simulator with an irradiation light intensity of 100 mW cm^{-2}. The external quantum efficiency (EQE) of the devices was measured by Solar Cell Spectral Response Measurement System QE-R3011 (Enli Technology CO., Ltd.). The light intensity at each wavelength was calibrated with a standard single-crystal Si photovoltaic cell.

Results and Discussions

Synthesis

As shown in **Scheme 1**, P(PDI-BDT-O) and **P(PDI-BDT-T)** were synthesized by Pd-catalyzed Stille-coupling reaction with a yield of 37% and 71%, respectively. The polymer shows good solubility in chlorinated solvents such as chloroform, chlorobenzene and *o*-dichlorobenzene (*o*-DCB). The number average molecular weight (M_n) and polydispersity index of polymers P(PDI-BDT-O) and **P(PDI-BDT-T)** are 17.3 K / 1.48 and 25.0 K / 1.7, respectively, which were estimated by high temperature gel permeation chromatography at 160 °C using 1,2,4-trichlorobenzene as the solvent and polystyrene with narrow molecular weight distribution as a standard.

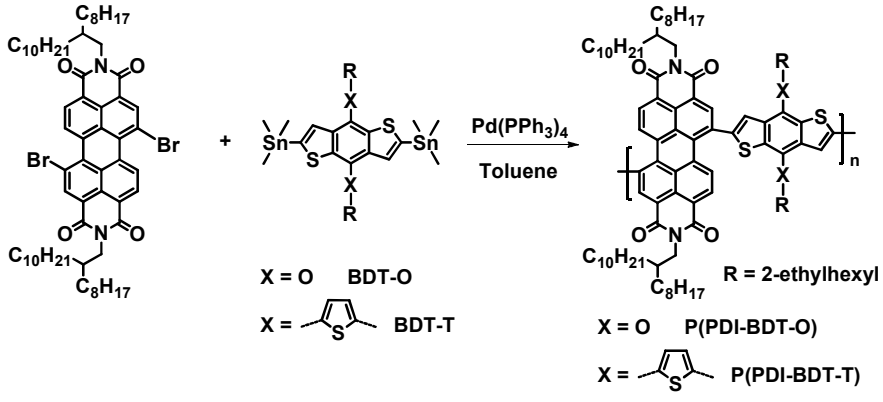

Scheme 1 Synthesis route of polymer P(PDI-BDT-O) and **P(PDI-BDT-T)**.

Thermal properties

The thermal stability of **P(PDI-BDT-T)** was analyzed by the thermogravimetric

analysis (TGA) as shown in **Fig. 2a**. **P(PDI-BDT-T)** shows a sufficiently high decomposition temperature of ca. 360 °C, indicating that the thermal stability is enough for the application as photovoltaic materials in PSCs. From the DSC thermograms of **P(PDI-BDT-T)** (**Fig. 2b**), no obvious exotherm or endotherm peaks were observed from 50 to 250 °C, at a heating rate of 10 °C/min, and mean that this polymer is amorphous.

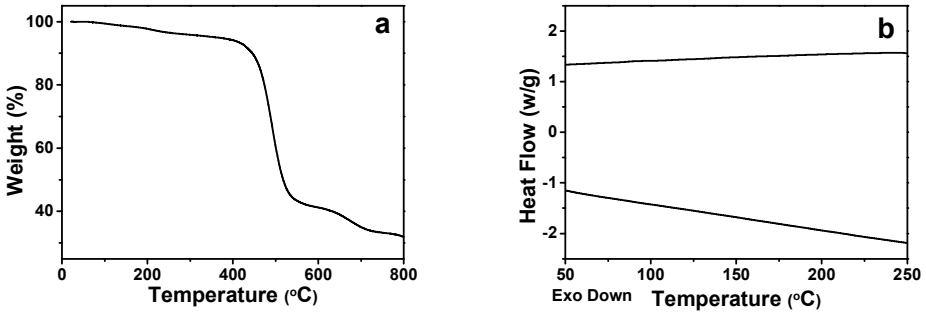

Fig. 2 TGA (a) and DSC (b) plots of **P(PDI-BDT-T)** with a heating rate of 10 °C/min under the inert atmosphere.

Absorption Spectra and Electronic Energy Levels

Fig. 3a shows the absorption spectra of the polymer donor and acceptors in thin films. The absorption spectrum of the polymer donor PTB7-Th film displays three main absorption peaks with λ_{max} at 483, 638 and 696 nm respectively. The polymer acceptors P(PDI-BDT-O) and **P(PDI-BDT-T)** films show three absorption peaks at 376, 537 and 649 nm / 385, 547 and 656 nm, respectively. The absorption spectrum of **P(PDI-BDT-T)** film red-shifted by ca. 10 nm than that of P(PDI-BDT-O), which could be ascribed to the introduction of the conjugated side chains in the 2D polymer

P(PDI-BDT-T). The absorption edges of P(PDI-BDT-O) and **P(PDI-BDT-T)** are at 748 and 757 nm, corresponding to an optical bandgap (E_g) of 1.66 and 1.64 eV, respectively. In addition, the absorption peaks of P(PDI-BDT-O) and **P(PDI-BDT-T)** show the similar stronger intensity at 350-450 nm, compared with that of PTB7-Th. Thus, the absorption spectra of PTB7-Th and P(PDI-BDT-O) or **P(PDI-BDT-T)** were complementary each other in the entire visible range.

The HOMO and LUMO energy levels of the conjugated polymers P(PDI-BDT-O) and **P(PDI-BDT-T)** were determined by electrochemical cyclic voltammetry (CV) of its thin film on working electrode.[42, 43] As shown in the cyclic voltammograms of P(PDI-BDT-O) and **P(PDI-BDT-T)** (see **Fig. 3b**), the onset reduction and oxidation potentials (E_{red} and E_{ox}) of P(PDI-BDT-O) and **P(PDI-BDT-T)** were -0.83 / 0.78 V and -0.82 / 0.99 V vs. Ag/Ag^+, respectively. Thus, in accordance with equations:[44] HOMO = -e (E_{ox} + 4.71) (eV); LUMO = -e (E_{red} + 4.71) (eV), HOMO and LUMO levels of P(PDI-BDT-O) and **P(PDI-BDT-T)** were calculated to be -5.47 / -3.88 eV and -5.70 / -3.89 eV, respectively. Obviously, the LUMO level of P(PDI-BDT-O) and **P(PDI-BDT-T)** with BDT as the donor unit in the polymers are up-shifted by ca. 0.1 eV, in comparison with that of the PDI-based *n*-type polymer with dithienothiophene as donor unit,[4] due to the better ionization potential of the functional groups BDT segment.[45] The higher LUMO energy level could be beneficial to high V_{oc} of all-PSCs with the polymer as acceptor, since V_{oc} of the PSCs is propotional to the difference of the LUMO of the acceptor and the HOMO of the donor.

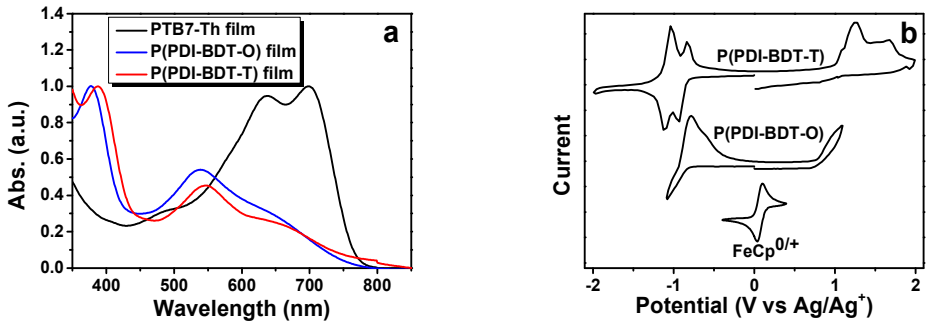

Fig. 3 (a) UV-vis absorption spectra of donor PTB7-Th, acceptors P(PDI-BDT-O) and **P(PDI-BDT-T)** in thin films; **(b)** Cyclic voltammograms of P(PDI-BDT-O) and **P(PDI-BDT-T)** films on a platinum electrode measured in 0.1 mol L^{-1} Bu_4NPF_6 acetonitrile solutions at a scan rate of 50 mV s^{-1}.

Photovoltaic Performance of All-PSCs

The photovoltaic properties of the polymer acceptor **P(PDI-BDT-T)** or P(PDI-BDT-O) are investigated by fabricating all-PSCs with PTB7-Th as donor and **P(PDI-BDT-T)** or P(PDI-BDT-O) as acceptor with the conventional device structure of ITO/PEDOT:PSS/PTB7-Th:**P(PDI-BDT-T)** or P(PDI-BDT-O)/Ca/Al, where ITO is indium tin oxide, PEDOT is poly(3,4-ethylenedioxythiophene), and PSS is poly(styrene sulfonate). Initially, we investigated the effect of the D/A weight ratios of PTB7-Th:**P(PDI-BDT-T)** on the photovoltaic performance of the all-PSCs. **Fig. 4a** shows the current density-voltage (J-V) curves of the devices with different D/A ratios (2:1, 1.5:1 and 1:1) under the illumination of AM 1.5G, 100 mW cm^{-2}. The photovoltaic parameters, including the short-circuit current density (J_{sc}), the

open-circuit voltage (V_{oc}), fill factor (FF), and PCE, are outlined in **Table 1**. Obviously, the optimal D/A ratio of the blend active layers is 1.5:1, the optimum efficiency of 4.31% is observed for the device based on PTB7-Th:**P(PDI-BDT-T)** (1.5:1, w/w) with J_{sc} of 11.06 mA cm^{-2}, V_{oc} of 0.80 V and FF of 48.6%. In terms of the optimum D/A blend ratio (1.5:1, w/w), the thermal annealing (100 ^{o}C and 120 ^{o}C) and solvent additive (DIO, CN, NMP) treatment[46, 47] were performed for further improving the photovoltaic performance. A slightly improved PCE of 4.71% was obtained with J_{sc} of 11.51 mA cm^{-2}, V_{oc} of 0.80 V and FF of 51.1% for the all-PSC with using 1 vol % CN (see **Fig. 4a**). While the PCE of the devices with the additive of 1 vol % DIO and 1 vol % NMP are 4.37% and 4.39%, respectively. However, the photovoltaic performance of the devices with thermal annealing decreased a little, the PCE of the PSCs with the thermal annealing at 100 ^{o}C or 120 ^{o}C for 10 min was 4.15% and 4.17%, respectively (see **Fig. S2** and **Table S1** in SI). The good photovoltaic performance (PCE of 4.71%) of the all-PSCs without the need of thermal annealing is an advantage of the polymer acceptor **P(PDI-BDT-T)**. While for the control polymer acceptor P(PDI-BDT-O), PCE of the all-PSC based on PTB7-Th:**P(PDI-BDT-O)** (1.5:1, w/w) is only 2.69% with a J_{sc} of 9.60 mA cm^{-2}, V_{oc} of 0.72 V, and FF of 38.8%. With the 1 vol % CN solvent additive treatment, PCE of the all-PSCs with **P(PDI-BDT-O)** as acceptor improved a little to 2.75% with a J_{sc} of 10.14 mA cm^{-2}, V_{oc} of 0.72 V, and FF of 37.6%. Obviously, the 2D-conjugated polymer **P(PDI-BDT-T)** exhibit better photovoltaic performance than the control 1D polymer P(PDI-BDT-O) when they are used as acceptor in all-PSCs.

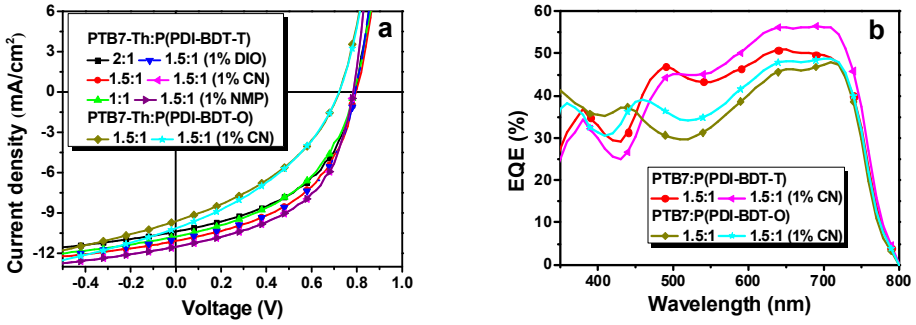

Fig. 4 (a) *J*−*V* curves of the PSCs based on PTB7-Th as donor and :**P(PDI-BDT-T)** or P(PDI-BDT-O) as acceptor with different D/A weight ratios (2:1, 1.5:1, 1:1) and different additive treatment; (b) EQE curves of the PSCs based on PTB7-Th:**P(PDI-BDT-T)** or PTB7-Th:P(PDI-BDT-O) (1.5:1, w/w) with or without 1% CN additive treatment, under the illumination of AM1.5G, 100 mW/cm^2.

Fig. 4b displays the external quantum efficiency (EQE) curves of the all-PSCs based on PTB7-Th:**P(PDI-BDT-T)** or PTB7-Th:P(PDI-BDT-O) (1.5:1, w/w). The EQE plots show a broad peak covering the wavelength range from 350 nm to ca. 800 nm, which is corresponding to the absorptions of both the polymer donor and the polymer acceptor. The enhanced EQE values at ca. 400 nm and in the range of 500-600 nm should be benefitted from the absorption of the polymer acceptor. In comparison of the EQE values of the PSCs based on PTB7-Th:**P(PDI-BDT-T)** without and with 1% CN additive, the maximum EQE value in the wavelength range of ca. 640~730 nm is enhanced from 52 % to 58%, which is consistant with the increased J_{sc} of the devices with the 1% CN additive treatment. The higher EQE values and larger J_{sc} values of the all-PSCs with **P(PDI-BDT-T)** as acceptor should

be benefitted from the stronger absorption in the long-wavelength range of 640-730 nm. The maximum EQE value of the PSC based on PTB7-Th:P(PDI-BDT-O) is 47% without solvent additive, and 49% with 1 vol % CN additive treatment. The EQE values agree well with the J_{sc} values obtained form *J-V* curves.

Table 1 Photovoltaic properties of the PSCs based on PTB7-Th:**P(PDI-BDT-T)** and PTB7-Th:P(PDI-BDT-O) with different D/A ratios and additives under the illumination of AM 1.5G, 100 mW cm^{-2}.

Acceptors	D/A (w/w)	Additives	V_{oc} (V)	J_{sc} (mA cm^{-2})	FF (%)	PCE (%)	Thickness (nm)
P(PDI-BDT-T)	2:1	w/o	0.79	10.37	47.5	3.89	98
	1.5:1	w/o	0.80	11.06	48.6	4.31	90
	1.5:1	1% DIO	0.80	10.99	49.6	4.37	80
	1.5:1	1% CN	0.80	11.51	51.1	4.71	85
	1.5:1	1% NMP	0.80	10.93	50.3	4.39	89
	1:1	w/o	0.79	10.75	45.8	3.88	93
P(PDI-BDT-O)	1.5:1	w/o	0.72	9.60	38.8	2.69	91
	1.5:1	1% CN	0.72	10.14	37.6	2.75	103

Charge carrier mobilities

In order to understand the effect of the D/A weight ratios of the active layer on the photovoltaic performance of the PSCs, the charge carrier mobilities were measured for the pure polymer **P(PDI-BDT-T)** or P(PDI-BDT-O) and the polymer blends of PTB7-Th:**P(PDI-BDT-T)** with different D/A ratios (2:1, 1.5:1 and 1:1, w/w), by

using the space-charge-limited current (SCLC) method. **Fig. 5** and **Fig. S4 in SI** show the current-voltage plots for the mobility measurements, and **Table 2** lists the hole and electron mobility values obtained from the measurements. It can be seen from **Table 2** that the electron mobility of pure **P(PDI-BDT-T)** and P(PDI-BDT-O) are 3.11×10^{-3} cm^2 V^{-1} s^{-1} and 1.66×10^{-3} cm^2 V^{-1} s^{-1}, respectively. Obviously, the electron mobility of **P(PDI-BDT-T)** film is superior to that of P(PDI-BDT-O) film, which could be ascribed to the introduction of thiophene conjugated side chain on its BDT unit. The electron mobility of pure **P(PDI-BDT-T)** is one order higher than that of the polymer blends with D/A weight ratios of 1.5:1 and 1:1 and two orders higher than that of the polymer blend with weight ratio of 2:1. The results indicate that blending PTB7-Th into **P(PDI-BDT-T)** disrupted the **P(PDI-BDT-T)** domains and influenced the electron pathway of the **P(PDI-BDT-T)** network, and too high PTB7-Th concentration in the blend film with D/A weight ratio of 2:1 decreased the electron mobility of the blend film significantly.[48, 49] Interestingly, the hole mobilities of the polymer blend films with weight ratios of 2:1, 1.5:1 and 1:1 are approximately in the same order of 10^{-2} cm^2 V^{-1} s^{-1}, less dependent on the D/A weight ratios. Obviously, it is very important to increase the electron mobility of the polymer blend films for further improving the photovoltaic performance of the all-PSCs.

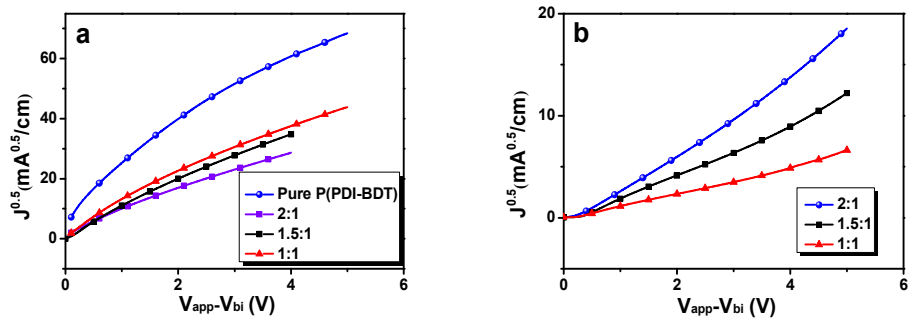

Fig. 5 The current-voltage plots of the electron-only devices (a) and hole-only devices (b) with different active layers for the mobility measurements.

Table 2 Hole and electron mobility values of the pure polymer **P(PDI-BDT-T)** or P(PDI-BDT-O) and the PTB7-Th:**P(PDI-BDT-T)** polymer blends with different D/A weight ratios measured by the SCLC method.

D/A	μ_e (cm^2/vs)	μ_h (cm^2/vs)
Pure P(PDI-BDT-T)	3.11×10^{-3}	-
Pure P(PDI-BDT-O)	1.66×10^{-3}	-
2:1	7.86×10^{-5}	3.99×10^{-2}
1.5:1	1.23×10^{-4}	2.76×10^{-2}
1:1	6.55×10^{-4}	1.01×10^{-2}

Morphology study

The morphology controlling of the active layer plays very important role in optimising the photovoltaic performance of the PSCs. For understanding the effect of the D/A weight ratios and solvent additive on the morphology of the active layers and on the photovoltaic performance of the all-PSCs, we measured the morphology of the polymer blend films with different D/A weight ratios and without or with different

solvent addtives. Atomic force microscopy (AFM) images of pure **P(PDI-BDT-T)** and the polymer blend films with different weight ratios, as shown in **Fig. S3** in SI, reveal that the surface roughness of the pure **P(PDI-BDT-T)** film is 0.48 nm, and that of the blends with weight ratios of 2:1, 1.5:1 and 1:1 are increased to 1.16, 1.33 and 1.29 nm, respectively. The results indicate that the surface roughness is less dependent on the D/A weight ratios in the polymer blend films in the all-PSCs. **Fig. 6** shows the AFM images of the PTB7-Th:**P(PDI-BDT-T)** blend films (1.5:1, w/w) without and with different additives. There is also no big difference of the surface morphology of the polymer blend films with different solvent additive treatment conditions.

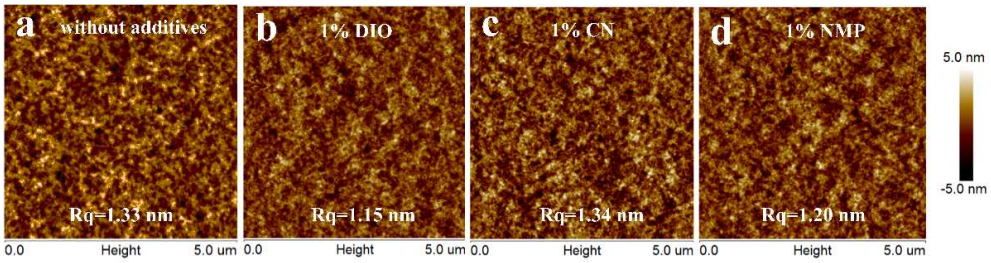

Fig. 6 AFM images of the PTB7-Th:**P(PDI-BDT-T)** blend films (1.5:1, w/w) without (a) and with additive treatment of (b) 1% DIO, (c) 1% CN and (d) 1% NMP.

We further studied the morphology of the polymer blend films by transmission electron microscopy (TEM). TEM images of PTB7-Th:**P(PDI-BDT-T)** blends with different weight ratios (2:1, 1.5:1 and 1:1, w/w) were shown in **Fig. S4** in SI. We found that TEM image of blend with the weight ratio of 1.5:1 displays the appropriate interpenetrating network morphology. Thus, higher PCE of the PSCs with the D/A

weight ratio of 1.5:1 agree with the results of the TEM images. **Fig. 7a-d** shows the TEM images of the blend films without and with the solvent treatment of 1 vol % DIO, 1 vol % CN and 1 vol % NMP, respectively. The polymer blend films without and with the solvent treatment of 1% DIO and 1% NMP display the similar morphologies according to the similar phase-separated size of light and dark domains (**Fig. 7a, b and d**). The TEM image of the blend film with 1 vol % CN solvent additive treatment shows a fibrous D/A interpenetrating network morphology with the fibrile size of ca. 10 nm (**Fig. 7c**), which should be beneficial to the increased J_{sc} and FF of the all-PSCs based on the active layer with the solvent treatment of 1% CN mentioned above.

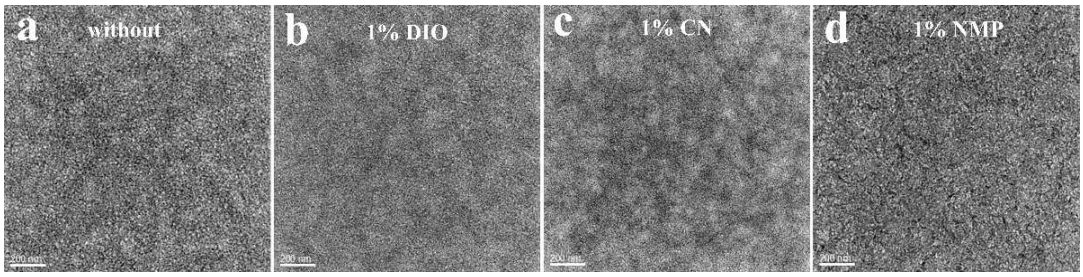

Fig. 7 TEM images of the PTB7-Th:**P(PDI-BDT-T)** blend films (1.5:1, w/w) without (a) and with solvent additive treatment of (b) 1% DIO, (c) 1% CN and (d) 1% NMP.

Conclusion

In this study, a *n*-type 2D-conjugated polymer, **P(PDI-BDT-T)**, is synthesized for the application as acceptor in all-PSCs. **P(PDI-BDT-T)** exhibits broad absorption in visible light range and its absorption spectrum is complementary with that of the

2D-conjugated polymer donor PTB7-Th. The LUMO level of **P(PDI-BDT-T)** is -3.89 eV which is slightly higher than that of the traditional acceptor PCBM, which is suitable for the application as acceptor in PSCs. The all-PSCs based on PTB7-Th:**P(PDI-BDT-T)** demonstrated a higher PCE of 4.71% at the optimized conditions with D/A weight ratio of 1.5:1 and with 1% CN additive treatment. The results of the charge carrier mobility measurements and the TEM images confirm the optimized device fabircation conditions of all-PSCs based on PTB7-Th:**P(PDI-BDT-T)** with D/A weight ratio of 1.5:1 and with solvent additive treatment of 1% CN. A corresponding 1D-conjugated polymer P(PDI-BDT-O) with alkoxy substituent on its BDT unit was also synthesized and applied as acceptor in all-PSCs for comparison with the 2D-conjugated polymer **P(PDI-BDT-T)**. PCE of the all-PSCs with P(PDI-BDT-O) as acceptor was only 2.75%, under the same experimental conditions. The results indicate that the 2D-conjugated *n*-type polymers with conjugated side chains on its donor unit could be promising polymer acceptors for all-PSCs.

Acknowledgements

This work was supported by the National Natural Science Foundation of China (91333204, 91433117, 51203168, 51422306), the Priority Academic Program Development of Jiangsu Higher Education Institutions, and the Strategic Priority Research Program of the Chinese Academy of Sciences (No. XDB12030200), the Postdoctoral research start-up funding of Soochow University (32317366, 32317400).

Notes and references

1 J. J. M. Halls, C. A. Walsh, N. C. Greenham, E. A. Marseglia, R. H. Friend, S. C. Moratti, A. B. Holmes, *Nature,* 1995, **376**, 498.

2 S. A. Jenekhe, S. Yi, *Appl. Phys. Lett.,* 2000, **77**, 2635.

3 M. M. Alam, S. A. Jenekhe, *Chem. Mater.,* 2004, **16**, 4647.

4 X. Zhan, Z. Tan, B. Domercq, Z. An, X. Zhang, S. Barlow, Y. Li, D. Zhu, B. Kippelen, S. R. Marder, *J. Am. Chem. Soc.,* 2007, **129**, 7246.

5 Z. Tan, E. Zhou, X. Zhan, X. Wang, Y. Li, S. Barlow, S. R. Marder, *Appl. Phys. Lett*., 2008, **93**, 073309.

6 E. Zhou, J. Cong, Q. Wei, K. Tajima, C. Yang, K. Hashimoto, *Angew. Chem. Int. Ed.,* 2011, **50**, 2799.

7 E. Ahmed, G. Ren, F. S. Kim, E. C. Hollenbeck, S. A. Jenekhe, *Chem. Mater.,* 2011, **23**, 4563.

8 C. R. McNeill, *Energy Environ. Sci.,* 2012, **5**, 5653.

9 T. Earmme, Y.-J. Hwang, N. M. Murari, S. Subramaniyan, S. A. Jenekhe, *J. Am. Chem. Soc.,* 2013, **135**, 14960.

10 T. Earmme, Y. J. Hwang, S. Subramaniyan, S. A. Jenekhe, *Adv. Mater.,* 2014, **26**, 6080.

11 H. Li, T. Earmme, G. Ren, A. Saeki, S. Yoshikawa, N. M. Murari, S. Subramaniyan, M. J. Crane, S. Seki, S. A. Jenekhe, *J. Am. Chem. Soc.,* 2014, **136**, 14589.

12 X. Guo, A. Facchetti, T. J. Marks, *Chem. Rev.,* 2014, **114**, 8943.

13 C. Mu, P. Liu, W. Ma, K. Jiang, J. Zhao, K. Zhang, Z. Chen, Z. Wei, Y. Yi, J. Wang, *Adv. Mater.,* 2014, **26**, 7224.

14 D. Mori, H. Benten, I. Okada, H. Ohkita, S. Ito, *Adv. Energy Mater.,* 2014, **4**, 1301006.

15 Y.-J. Hwang, T. Earmme, B. A. E. Courtright, F. N. Eberle, S. A. Jenekhe, *J. Am. Chem. Soc.,* 2015, **137**, 4424.

16 J. W. Jung, J. W. Jo, C. C. Chueh, F. Liu, W. H. Jo, T. P. Russell, A. K. Y. Jen, *Adv. Mater.,* 2015, **27**, 3310.

17 K. D. Deshmukh, T. Qin, J. K. Gallaher, A. C. Y. Liu, E. Gann, K. O'Donnell, L. Thomsen, J. M. Hodgkiss, S. E. Watkins, C. R. McNeill, *Energy Environ. Sci.,* 2015, **8**, 332.

18 C. Lee, H. Kang, W. Lee, T. Kim, K. H. Kim, H. Y. Woo, C. Wang, B. J. Kim, *Adv. Mater.,* 2015, **27**, 2466.

19 C. Li, H. Wonneberger, *Adv. Mater.*, 2012, **24**, 613.

20 E. Kozma, M. Catellani, *Dyes and Pigments*, 2013, **98**, 160.

21 E. Zhou, K. Tajima, C. Yang, K. Hashimoto, *J. Mater. Chem.*, 2010, **20**, 2362.

22 E. Zhou, J. Cong, M. Zhao, L. Zhang, K. Hashimoto, K. Tajima, *Chem. Commun.*, 2012, **48**, 5283.

23 E. Zhou, J. Cong, K. Hashimoto, K. Tajima, *Adv. Mater.*, 2013, **25**, 6991.

24 Y. J. Hwang, B. A. E. Courtright, A. S. Ferreira, S. H. Tolbert, S. A. Jenekhe, *Adv. Mater.*, 2015, DOI: 10.1002/adma.201501604.

25 X. Wang, J. Huang, K. Tajima, B. Xiao, E. Zhou, *Mater. Today. Commun.*, 2015, **4**, 16.

26 Y. Zhou, T. Kurosawa, W. Ma, Y. Guo, L. Fang, K. Vandewal, Y. Diao, C. Wang, Q. Yan, J. Reinspach, J. Mei, A. L. Appleton, G. I. Koleilat, Y. Gao, S. C. B. Mannsfeld, A. Salleo, H. Ade, D. Zhao, Z. Bao, *Adv. Mater.,* 2014, **26**, 3767.

27 R. Duan, L. Ye, X. Guo, Y. Huang, P. Wang, S. Zhang, J. Zhang, L. Huo, J. Hou, *Macromolecules,* 2012, **45**, 3032.

28 X. Guo, M. Zhang, W. Ma, L. Ye, S. Zhang, S. Liu, H. Ade, F. Huang, J. Hou, *Adv. Mater.,* 2014, **26**, 4043.

29 H. J. Son, W. Wang, T. Xu, Y. Liang, Y. Wu, G. Li, L. Yu, *J. Am. Chem. Soc.,* 2011, **133**, 1885.

30 M. Zhang, X. Guo, W. Ma, S. Zhang, L. Huo, H. Ade, J. Hou, *Adv. Mater.,* 2014, **26**, 2089.

31 Y. Zhang, L. Gao, C. He, Q. Sun, Y. Li, *Polym. Chem.,* 2013, **4**, 1474.

32 X. Guo, M. Zhang, L. Huo, F. Xu, Y. Wu, J. Hou, *J. Mater. Chem.,* 2012, **22**, 21024.

33 L. Ye, S. Zhang, L. Huo, M. Zhang and J. Hou, *Acc. Chem. Res.,* 2014, **47**, 1595.

34 M. Zhang, X. Guo, Y. Li, *Macromolecules,* 2011, **44**, 8798.

35 D. Qian, L. Ye, M. Zhang, Y. Liang, L. Li, Y. Huang, X. Guo, S. Zhang, Z. Tan, J. Hou, *Macromolecules,* 2012, **45**, 9611.

36 Z. Yuan, Y. Xiao, Y. Yang, T. Xiong, *Macromolecules,* 2011, **44**, 1788.

37 F. Würthner, V. Stepanenko, Z. Chen, C. R. Saha-Möller, N. Kocher, D. Stalke, *J. Org. Chem.*, 2004, **69**, 7933.

38 P. Rajasingh, R. Cohen, E. Shirman, L. J. W. Shimon, B. Rybtchinski, *J. Org. Chem.*, 2007, **72**, 5973.

39 L. D. Wescott, D. L. Mattern, *J. Org. Chem.*, 2003, **68**, 10058.

40 L. Huo, S. Zhang, X. Guo, F. Xu, Y. Li, J. Hou, *Angew. Chem. Int. Ed.,* 2011, **50**, 9697.

41 S. Zhang, L. Ye, Q. Wang, Z. Li, X. Guo, L. Huo, H. Fan, J. Hou, *J. Phys. Chem. C*, 2013, **117**, 9550.

42 Y. Li, Y. Cao, J. Gao, D. Wang, G. Yu, A. J. Heeger, *Synth. Met.,* 1999, **99**, 243.

43 J. Hou, Z. a. Tan, Y. Yan, Y. He, C. Yang, Y. Li, *J. Am. Chem. Soc.,* 2006, **128**, 4911.

44 Q. Sun, H. Wang, C. Yang, Y. Li, *J. Mater. Chem.,* 2003, **13**, 800.

45 L. Dou, J. Gao, E. Richard, J. You, C.-C. Chen, K. C. Cha, Y. He, G. Li, Y. Yang, *J. Am. Chem. Soc.,* 2012, **134**, 10071.

46 X. Guo, M. Zhang, C. Cui, J. Hou, Y. Li, *ACS Appl. Mater. Interfaces,* 2014, **6**, 8190.

47 X. Guo, C. Cui, M. Zhang, L. Huo, Y. Huang, J. Hou, Y. Li, *Energy Environ. Sci.,* 2012, **5**, 7943.

48 M. M. Mandoc, W. Veurman, L. J. A. Koster, M. M. Koetse, J. Sweelssen, B. de Boer, P. W. M. Blom, *J. Appl. Phys.,* 2007, **101**, 104512.

49 H. Kang, K.-H. Kim, J. Choi, C. Lee, B. J. Kim, *ACS Macro Lett.,* 2014, **3**, 1009.